IMPROVED REVERBERATION TIME CONTROL FOR FEEDBACK DELAY NETWORKS

Karolina Prawda, Vesa Välimäki [*]

Acoustics Lab, Dept. of Signal Processing and Acoustics
Aalto University
Espoo, Finland
karolina.prawda@aalto.fi

Sebastian J. Schlecht

International Audio Laboratories[†]
Erlangen, Germany

sebastian.schlecht@audiolabs-erlangen.de

ABSTRACT

Artificial reverberation algorithms generally imitate the frequency-dependent decay of sound in a room quite inaccurately. Previous research suggests that a 5% error in the reverberation time (T60) can be audible. In this work, we propose to use an accurate graphic equalizer as the attenuation filter in a Feedback Delay Network reverberator. We use a modified octave graphic equalizer with a cascade structure and insert a high-shelf filter to control the gain at the high end of the audio range. One such equalizer is placed at the end of each delay line of the Feedback Delay Network. The gains of the equalizer are optimized using a new weighting function that acknowledges nonlinear error propagation from filter magnitude response to reverberation time values. Our experiments show that in real-world cases, the target T60 curve can be reproduced in a perceptually accurate manner at standard octave center frequencies. However, for an extreme test case in which the T60 varies dramatically between neighboring octave bands, the error still exceeds the limit of the just noticeable difference but is smaller than that obtained with previous methods. This work leads to more realistic artificial reverberation.

1. INTRODUCTION

Reverberation time is one of the most important parameter used to determine the acoustic quality of physical spaces. Multiple studies have been conducted to evaluate the accuracy of perceiving the changes in the reverberation time for various types of signals. Seraphim [1] determined the just noticeable difference (JND) of the reverberation time to be 5%. However, more recent studies showed that for bandlimited noise the difference is perceivable only when it exceeds 24% of the target value [2], compared to 5% to 7% for impulse signals and 3% to 9% for reverberated speech [3]. The JND of 5% is used in this work to comply with the current ISO standard [4].

Various algorithms are used to produce artificial reverberation, with the Feedback Delay Network (FDN) being currently among the most popular ones [5–7]. The first objective in designing an FDN is to make it lossless. Attenuation filters are introduced to achieve target energy decay. Over time, various types of attenuation filters have been proposed. Initially, a first-order lowpass infinite impulse response (IIR) filter was used because of its low computational cost and ease of design [5, 8]. Later, biquadratic filters were introduced allowing to control the decay time in three independent frequency bands with adjustable crossover frequencies [9]. In [10], a 13th-order filter comprising single bandpass filters as described in [11] and a second-order Butterworth bandpass filter was proposed.

The most advanced method of controlling decay time in artificial reverberation in several frequency bands uses a proportional graphic equalizer [12]. This method was recently improved by Schlecht and Habets, who determined the filter parameters by solving the nonlinear least-squares problem with linear constraints approximating the target reverberation-time response directly [13]. This approach offered very accurate control of decay time and ensured that the FDN remained stable. However, the computation of filter parameters proved to be inefficient, especially in real-time applications [13].

The present work proposes an accurate method to control reverberation time in octave bands utilizing attenuation filters that produce small approximation errors. It is an extension to previous work done by Schlecht and Habets [13]. This paper introduces a novel graphic equalizer (GEQ) with an additional high-shelf filter as an attenuation filter inside the FDN and presents a weighted-gain optimization method that acknowledges nonlinear error propagation from filter magnitude response to reverberation time values. The paper is organized as follows. Section 2 discusses attenuation filters and proposes a new design as well as a weighted-gain optimization method. Section 3 presents case studies in which we test the proposed method and compare the proposed design to other solutions in terms of the approximation error as well as computational cost. Section 4 summarizes the work presented in the paper, gives conclusions about the results, and proposes ideas for future research.

2. ATTENUATION FILTER

An FDN is a comb filter structure with multiple delay lines interconnected by a feedback matrix [5]. When designing FDNs, the first step is to make it lossless, ensuring that the energy will not decay for any possible type of delay [7]. The frequency-dependent reverberation time can then be implemented by inserting an attenuation filter at the beginning or at the end of each delay line. As the filters do not work in relation to one another and are only dependent on their corresponding delay line, they can be analyzed separately. Instead of the FDN, we can analyze the simpler single-delay-line absorptive feedback comb filter, i.e.,

$$H(z) = \frac{1}{1 - A(z)z^{-L}}, \tag{1}$$

[*] This work was supported by the "Nordic Sound and Music Computing Network—NordicSMC", NordForsk project number 86892.

[†] The International Audio Laboratories Erlangen are a joint institution of the Friedrich-Alexander-Universität Erlangen-Nürnberg (FAU) and Fraunhofer Institut für Integrierte Schaltungen IIS.

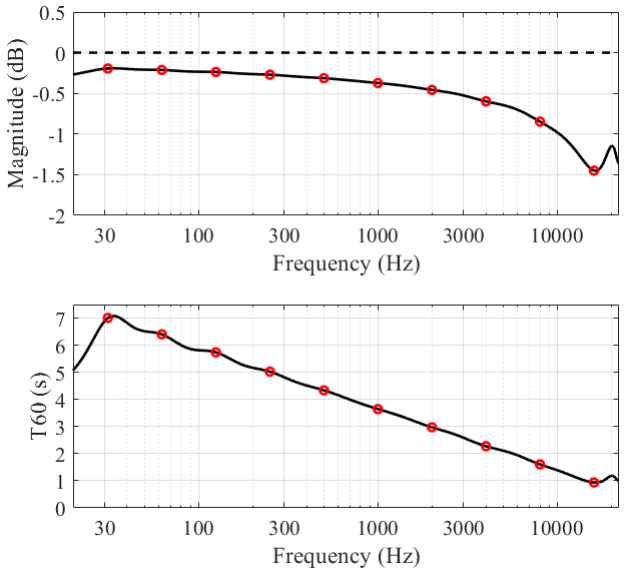

Figure 1: *Relationship between (top) gain-per-sample and (bottom) resulting reverberation time for the delay-line length of* $L = 1000$ *samples. Red markers indicate the octave bands. The horizontal dashed line in the top figure is the unit-gain limit, reaching which would lead to an infinite reverberation time.*

where L is the delay length in samples and $A(z)$ is the transfer function of the attenuation filter. For further analysis of the magnitude in dB, the attenuation filter is given by

$$A_{\text{dB}}(\omega) = 20 \log_{10} |A(e^{j\omega})|, \tag{2}$$

where $\omega = 2\pi f / f_{\text{s}}$ is the normalized frequency, f is the frequency in Hz, and f_{s} is the sampling rate in Hz. Such a filter should be designed to approximate the gain-per-sample necessary to obtain the desired frequency-dependent reverberation time, $T_{60}(\omega)$. This gain in dB is expressed as

$$\gamma_{\text{dB}}(\omega) = \frac{-60}{f_{\text{s}} T_{60}(\omega)}, \tag{3}$$

where $T_{60}(\omega)$ is in seconds. The gain is dependent on the delay-line length, growing proportionally to the number of delay samples L. As a result, longer delay lines decay faster than short ones. To obtain the target gain and, as a consequence, the desired frequency-dependent reverberation time, the following condition should be met:

$$A_{\text{dB}}(\omega) = L \gamma_{\text{dB}}(\omega). \tag{4}$$

Fig. 1 illustrates the relation between the gain-per-sample values of the single-delay-line absorptive feedback comb filter as presented in Eq. (1) with the attenuation filter designed according to Eq. (2-4) and the resulting $T_{60}(\omega)$ values. The delay-line length was set to $L = 1000$ samples and the target reverberation time was set to decrease linearly in octave bands from 7 s at 31.5 Hz to 1 s at 16 kHz.

2.1. Graphic equalizer design

The attenuation filter in the present work is realized with the cascade GEQ, composed of second-order IIR peak-notch filters proposed by Orfanidis [14] and designed using a method proposed by

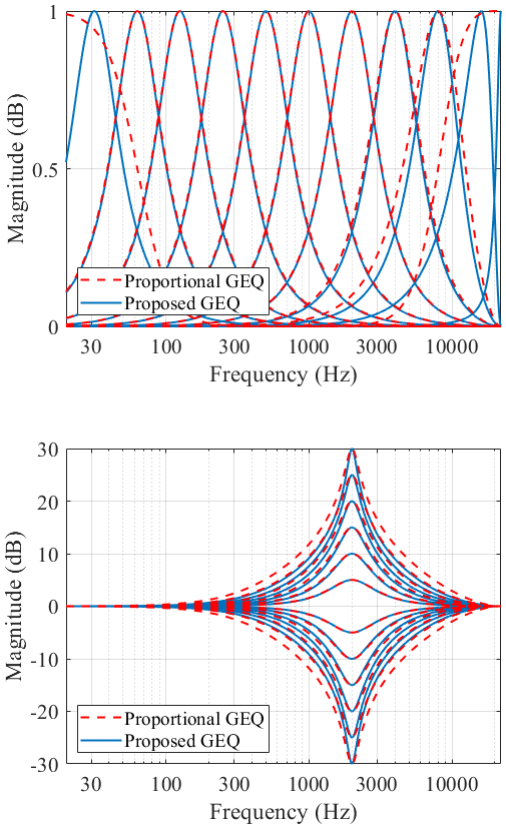

Figure 2: *Comparison of magnitude responses of the proposed GEQ with a high-shelf filter to the proportional graphic equalizer used in [13]. Top: magnitude responses for individual biquadratic filters and a prototype gain of 1 dB for ten frequency bands. Bottom: Single-band proportional gain behavior of the magnitude response.*

Välimäki and Liski [15], where extra frequency points are added and one iteration step is used to obtain a highly accurate magnitude response. The GEQ is also composed of only peak-notch filters, as opposed to the usual approach in which shelf filters are applied to the highest and lowest frequency bands. Using only peak-notch filters improves the symmetry of the magnitude responses of individual filters and the accuracy of the equalizer. This results in the proposed design producing approximation errors of less than ± 1 dB for command gains within a range of -12 to $+12$ dB [15]. The top plot of Fig. 2 depicts the magnitude responses of the individual biquadratic filters of the proposed GEQ, with an additional high-shelf filter as described in Sec. 2.2., compared to the proportional graphic equalizer from [13]. The approach adopted in the present paper displays more symmetrical magnitude responses even for high frequencies. The bottom plot of Fig. 2 presents the magnitude response of peak-notch filters for command gains between -30 and $+30$ dB.

The transfer function of a GEQ with M bands is given by

$$H(e^{j\omega}) = G_0 \prod_{m=1}^{M} H_{\text{m}}(e^{j\omega}), \tag{5}$$

where G_0 is the overall broadband gain factor and $H_{\text{m}}(e^{j\omega})$ are

the frequency responses of equalizing filters ($m = 1, 2, 3..., M$). The corresponding response in dB can be written as

$$H_{\text{dB}}(e^{j\omega}) = g_0 + \sum_{m=1}^{M} H_{\text{dB,m}}(e^{j\omega}). \tag{6}$$

For the accurate approximation of the reverberation time T_{60} over a broad frequency range, the command gains are defined for ten octave bands, having center frequencies ranging from 31.5 Hz to 16 kHz. This results, however, in the magnitude approaching 0 dB quite dramatically outside the considered frequency range. The reverberation time approximated for the octave bands below 31.5 Hz and above 16 kHz can appear to be very long, which may affect whole decay, preventing it from ever reaching -60 dB. To avoid this situation, we propose that the command gains be first shifted up to decrease their distance from zero and after the gain optimization, the entire magnitude response be scaled down by the same amount as for scaling up. This is depicted in the top and middle panes of Fig. 3. This yields the following changes to Eq. (6):

$$\widetilde{H}_{\text{dB}}(e^{j\omega}) = g_0 + \sum_{m=1}^{M} (H_{\text{dB,m}}(e^{j\omega}) - \frac{g_0}{M}). \tag{7}$$

In this way, the rise in magnitude at frequencies below 31.5 Hz and above 16 kHz are less steep. The shifting and scaling value can be set to the median of all command gains, as suggested in [16]. This also smooths the frequency response, causing very little ripple, as seen in the filter response comparison with and without scaling in Fig. 4.

2.2. High-shelf filter

In physical room acoustics, the decay time at high frequencies is usually shorter than at low frequencies, thus making the corresponding command gains considerably lower at high frequencies. Therefore, the operation of scaling and shifting the gains by the median may not be sufficient to prevent the magnitude from quickly approaching large values for frequencies above 16 kHz. For this reason, we use a first-order high-shelf filter implemented as suggested in [17] to equalize the problematic high frequencies. The gain of the shelf filter is set to the gain of the highest considered octave band, and the crossover frequency is set to 20.2 kHz. The latter value was experimentally found to introduce the smallest error in the reverberation time at 16 kHz.

The shelf filter introduces considerable ripple in the equalizer response above the frequency range of interest, but since it occurs at very high frequencies and the resulting reverberation time is much shorter than at lower frequencies, it is assumed to be inaudible. The response of the GEQ with the shelf filter is shown in the bottom pane of Fig. 3.

2.3. Filter-gain optimization

A common flaw in graphic equalizers is the interaction occurring between neighboring peak-notch filters, causing the response of each filter leak to other center frequencies [15–17]. A K-by-N interaction matrix $\mathbf{B}$ that shows this effect and stores the normalized amplitude response in dB of all M filters at K control frequency points is given by:

$$B_{k,m} = H_{\text{dB},m}(e^{j\omega_k})/g_{\text{p},m}, \tag{8}$$

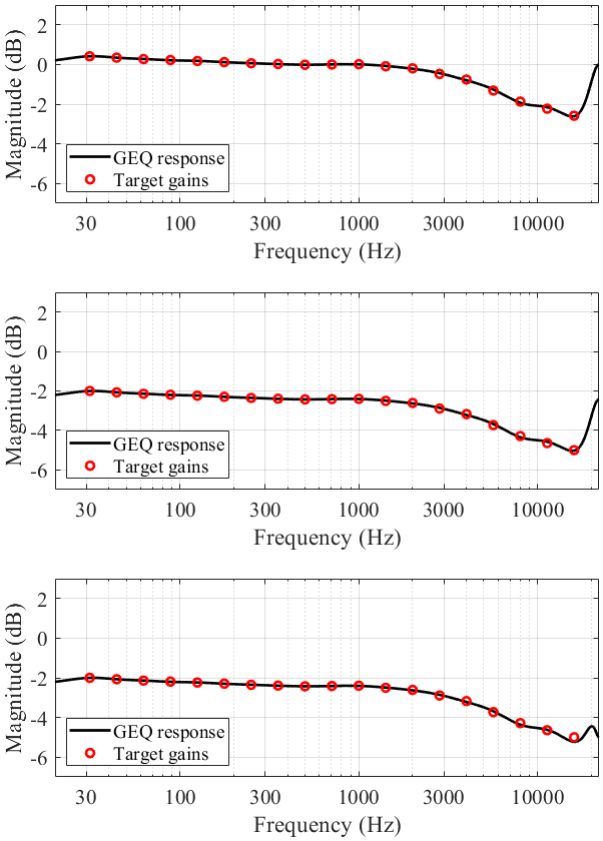

Figure 3: *Stages of obtaining the final frequency response of the GEQ for a delay length of 100 ms. (Top) Gains shifted up by their median value. (Middle) Gains scaled by a constant value. (Bottom) A high-shelf filter inserted to attenuate frequencies above 16 kHz.*

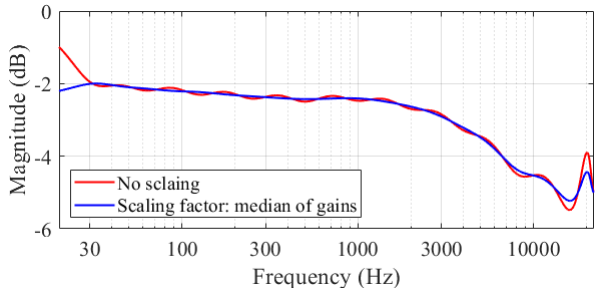

Figure 4: *Frequency response of the GEQ for a delay length of 100 ms, shifted and scaled by the median of gains compared to the response without scaling.*

where $k = 1, 2, ...K$ are control frequency points, $m = 1, 2, ...M$ are filter indices, and $\mathbf{g}_{\text{p}} = \left[g_{\text{p},1}, g_{\text{p},2}, ..., g_{\text{p,m}},\right]^T$, where $(.)^T$ denotes the transpose, is the vector of prototype dB gains common to all equalizing filters. The interaction matrix of the proposed GEQ for $K = 100$ and $N = 11$ is shown in Fig. 5. As a consequence of leakage, the magnitude response of the equalizer depends on the values stored in the interaction matrix. Considering that the GEQ is used as the attenuation filter in the FDN, Eq. (4) can now be

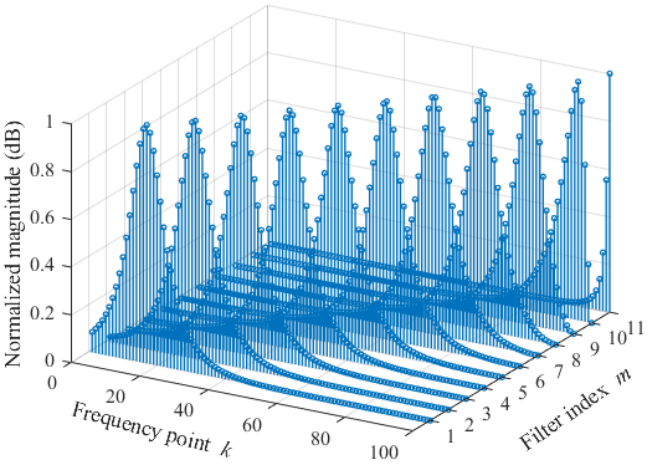

Figure 5: *A* 100*-by-*11 *interaction matrix of the proposed GEQ that stores the normalized amplitude of each filter that leaks to neighboring frequency points.*

expressed as

$$A_{\mathrm{dB}}(\boldsymbol{\omega}) = \mathbf{B}\mathbf{g}_{\mathrm{p}}, \tag{9}$$

where $\boldsymbol{\omega}$ is a $K \times 1$ vector of control frequencies.

2.4. Weighted-gain optimization

The GEQ used in the present work approximates the command gains strictly within 1 dB. However, in some instances of the reverberation time changing dramatically for neighboring octave bands, the differences in the command gains may be too high for the resulting filter magnitude response to follow without producing much error. Therefore, a method for gain optimization is introduced.

The approximation of the target magnitude response can be done on the dB scale by minimizing the error norm based on Eq. (4):

$$\|A_{\mathrm{dB}}(\boldsymbol{\omega}) - L\gamma_{\mathrm{dB}}(\boldsymbol{\omega})\|_2^2. \tag{10}$$

This approach assumes that the error propagates to the resulting reverberation time linearly. In reality, the reverberation time is affected in a nonlinear fashion: a small error in the filter magnitude response, when the attenuation is weak and the gain close to 0 dB, causes much greater changes in the resulting reverberation time than the same error, when the attenuation is strong and the gain much smaller than 0 dB [13].

This problem can be overcome by directly minimizing the squared error in the resulting reverberation time, as suggested earlier in [13]:

$$E = \left\| \frac{1}{A_{\mathrm{dB}}(\boldsymbol{\omega})} - \frac{1}{L\gamma_{\mathrm{dB}}(\boldsymbol{\omega})} \right\|_2^2. \tag{11}$$

Alternatively, we can minimize the relative error between the filter and the target reverberation time:

$$\widetilde{E} = \left\| 1 - \frac{A_{\mathrm{dB}}(\boldsymbol{\omega})}{L\gamma_{\mathrm{dB}}(\boldsymbol{\omega})} \right\|_2^2. \tag{12}$$

When the weighting matrix $\mathbf{W}$ is defined as

$$\mathbf{W} = \mathrm{diag}\left(\frac{1}{L\gamma_{\mathrm{dB}}(\boldsymbol{\omega})} \right), \tag{13}$$

the relative error from Eq. (12) becomes

$$\widetilde{E} = \left\| 1 - \mathbf{W}A_{\mathrm{dB}}(\boldsymbol{\omega}) \right\|_2^2, \tag{14}$$

where the role of the weighting matrix $\mathbf{W}$ is to mimic the nonlinear behavior with a linear approximation in the sense of emphasizing the approximation error occurring close to 0 dB.

Error minimization was also performed by solving the linear problem using the Taylor-series approximation presented in [18]. However, since the method operates on a linear scale, as opposed to the suggested design which operates on the dB scale, no relevant improvement was observed. Therefore the method utilizing the Taylor-series approximation was not implemented further in the present work.

3. EVALUATION

The present work proposes to perform reverberation time approximation using a GEQ with weighted-gain optimization that minimizes the relative error between filter response and target reverberation time values. In order to evaluate that algorithm, two case studies were conducted. The first was aimed to reproduce the reverberation time of Promenadi Hall, a multipurpose hall located in Promenadikeskus in Pori. The second was conducted using a predefined reverberation time that differs considerably between neighboring octave bands to reveal potential weak spots of the algorithm and provide a valid comparison to the previous work. For both cases, the algorithm was tested with three lengths of delay lines: 10 ms, 50 ms, and 100 ms. The performance of the proposed algorithm was compared to the previous method of reverberation-time control in FDN presented in [13]. The computational cost measured in the number of operations per output sample with relation to other graphic equalizers was also examined.

3.1. Promenadi Hall

In the first case, the aim was to approximate the reverberation time of an existing architectural object. The target values were defined for octave bands and are presented in Table 1. The command gains for the GEQ were calculated based on these values. Fig. 6 compares the target magnitude response needed to obtain the desired reverberation time and the response of the GEQ for the delay-line lengths of 10, 50, and 100 ms.

The target magnitude response is followed by the response of the filter very accurately in every octave band it was specified in. The magnitude response below 31.5 Hz approaches the median value for the command gains, which was set as the equalizer's broadband gain. The only visible ripple of 0.02 dB, 0.11 dB and 0.23 dB for delay-line lengths of 10 ms, 50 ms and 100 ms, respectively, occur at very high frequencies, above 16 kHz, and is caused by the high-shelf filter.

The resulting reverberation time was calculated based on the magnitude response of the GEQ by converting it to dB using Eq. (2), and then using the condition from Eq. (4) to obtain the gain-per-sample in dB. The values of $T_{60}(\omega)$ were acquired based on Eq. (3) and are depicted in the top plot of Fig. 7 together with target values from Promenadi Hall. The obtained reverberation follows the behavior of the filter response, approximating the desired values very closely not only in the octave frequencies, but also in the entire frequency range. Although the values were calculated for three different delay-line lengths, the results do not vary visibly from each

Table 1: *Reverberation time values and error percentage for octave frequencies for Promenadi Hall. DL stands for delay length.*

Center frequency	31.5 Hz	63 Hz	125 Hz	250 Hz	500 Hz	1 kHz	2 kHz	4 kHz	8 kHz	16 kHz
Reverberation time	3.00 s	2.80 s	2.68 s	2.55 s	2.47 s	2.50 s	2.30 s	1.89 s	1.40 s	1.20 s
Error for DL of 10 ms	0.12%	0.03%	0.09%	0.05%	0.02%	0.35%	0.79%	1.00%	1.51%	4.43%
Error for DL of 50 ms	0.12%	0.03%	0.09%	0.05%	0.02%	0.35%	0.79%	1.00%	1.53%	4.44%
Error for DL of 100 ms	0.12%	0.03%	0.09%	0.05%	0.02%	0.35%	0.79%	0.99%	1.56%	4.50%

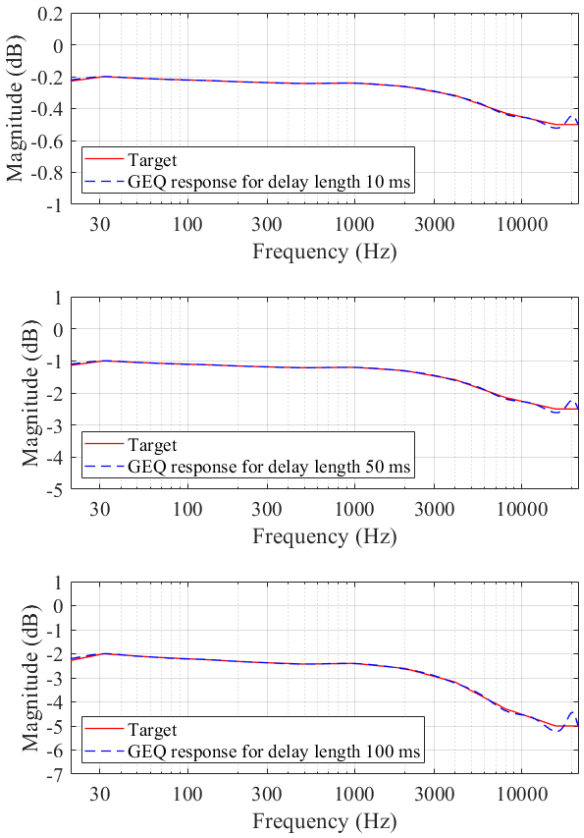

Figure 6: *Target magnitude response and response of the GEQ with first-order high-shelf filter for the case of Promenadi Hall in Pori.*

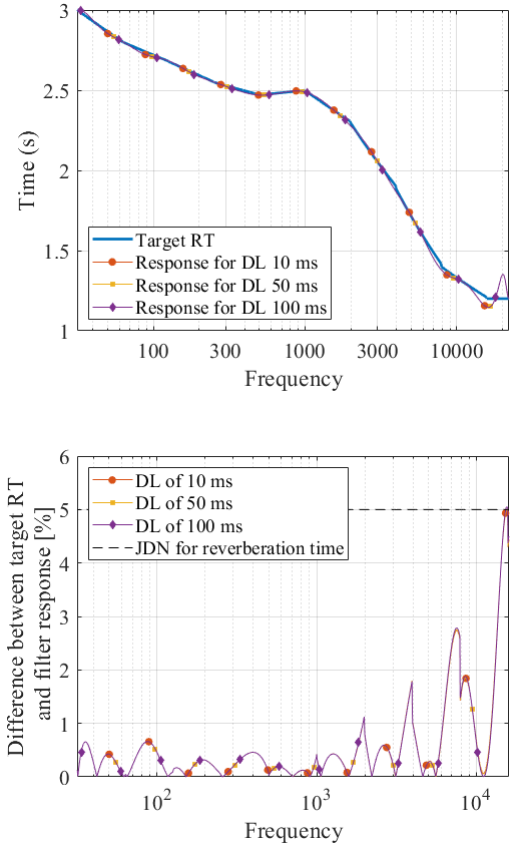

Figure 7: *(Top) Target reverberation time from Promenadi Hall and the values approximated by the GEQ. (Bottom) The difference expressed as percent of obtained reverberation time deviation from target values. RT is reverberation time.*

other, with the biggest difference between them reaching 0.07%. This proves that the proposed method works well regardless of the delay chosen when designing the FDN. This is also confirmed by the error values shown in Table 1, none of which exceed 5%, making the difference unnoticeable. Further evidence for the method's efficiency to accurately approximate reverberation time is in the bottom plot of Fig. 7, which shows the difference between the target and the obtained reverberation time for the whole frequency range.

The results obtained with the GEQ introduce deviations no bigger than 5% from the target value and therefore we refrained from trying to minimize the error.

3.2. Artificial extreme case

The second case was tested with predefined reverberation time values, which were aimed at being similar to those in [13]. Although in [13] the reverberation time values for octave bands were generated randomly, we decided to specify them manually in order to ensure the same tendency, which provides a good reference point for comparison of the two methods and is able to reveal shortcomings of the proposed design. The values of the reverberation time for octave frequencies are shown in Table 2.

The filters' magnitude responses obtained based on the desired decay are presented in Fig. 8. The target response is generally followed accurately. However, large differences in the reverberation between 2 kHz and 4 kHz cause a slight overshoot in magnitude for frequencies between 1 kHz and 2 kHz, which at its highest point

Table 2: *Reverberation time and error on octave frequencies for the artificial extreme case. Errors exceeding JND of 5.0% are highlighted.*

Center frequency	31.5 Hz	63 Hz	125 Hz	250 Hz	500 Hz	1 kHz	2 kHz	4 kHz	8 kHz	16 kHz
Reverberation time	1.00 s	1.00 s	1.00 s	1.00 s	1.00 s	3.00 s	3.00 s	0.25 s	1.00 s	1.00 s
Error for DL of 10 ms	0.12%	0.09%	0.17%	0.07%	3.66%	**12.59%**	**11.47%**	0.38%	2.96%	**5.80%**
Error for DL of 50 ms	0.13%	0.07%	0.22%	0.12%	3.11%	**8.79%**	**15.59%**	2.62%	**5.42%**	4.42%
Errorfor DL of 100 ms	0.15%	0.02%	0.39%	0.50%	1.52%	0.35%	**24.41%**	**6.03%**	**11.12%**	0.77%

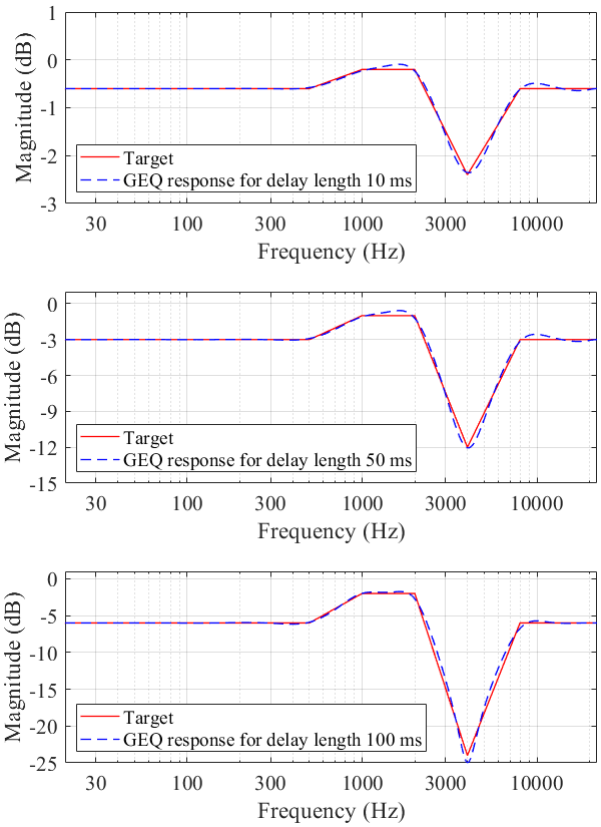

Figure 8: *Target magnitude response and response of the GEQ for three different delay-line lengths for the artificial extreme case.*

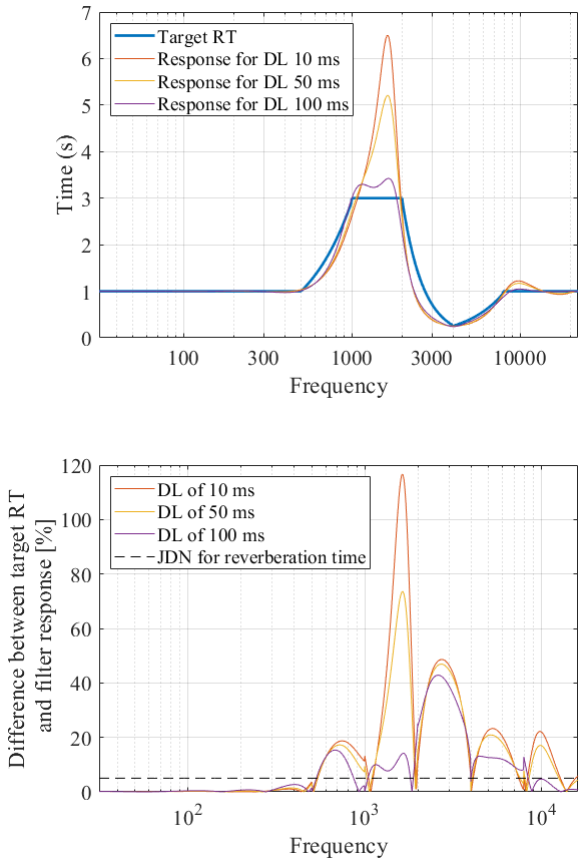

Figure 9: *(Top) Target reverberation time and reverberation time obtained with the GEQ for three different delay-line lengths for the artificial extreme case. (Bottom) The difference expressed as a percent of the obtained reverberation time deviation from target values.*

lies very close to zero. This causes a huge increase in the reverberation time for those frequencies, which is seen in the top plot in Fig. 9. When the difference between the target and the approximated reverberation time is expressed as a percentage into percentage, as shown in the bottom plot in Fig. 9, the 5% JND threshold is exceeded everywhere except for the low frequencies, where the target decay is the same in neighboring octave bands.

The results in Fig. 9 show the effect of the delay-line length on the approximation error. The attenuation for the shortest delay line is the weakest, making all deviations from the target magnitude to cause much error in the resulting reverberation time values. For the longest delay-line length, the overshoots between 1 kHz and 2 kHz, as well as around 8 kHz, are the smallest.

In order to improve the resulting reverberation time, we applied the gain-optimization method proposed in Sec. 2.3 by minimizing the error norm in Eq. (14) and using the weighting matrix in Eq. (13). The magnitude response of the GEQ is presented in Fig. 10. Overshoots between 1 kHz and 2 kHz were decreased at the cost of lower accuracy in approximating the target at 4 kHz. Additionally, some ripple was introduced in the frequency range between 250 Hz and 500 Hz.

The corresponding reverberation time values are shown in Fig. 11. The values that exceed the target the most were successfully reduced. The improvement was made without an unreasonable increase in error in the reverberation time for less problematic frequencies. Fig. 11 shows that the deviation in percent from the target values was the same or less for frequencies over 500 Hz. The error for low frequencies increased slightly, in most octave bands not exceeding the 5% JND.

The error-minimization method worked well for every delay-

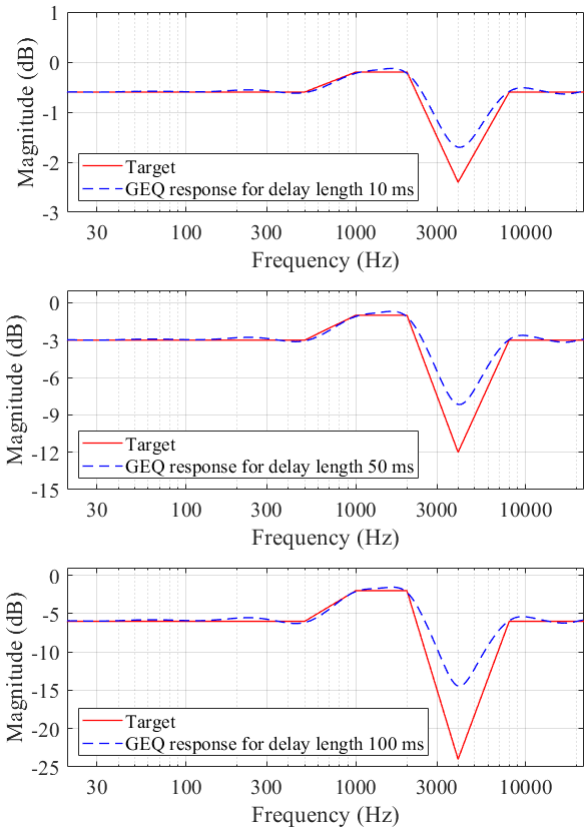

Figure 10: *Target magnitude response and response of the GEQ for three different delay-line lengths for the artificial extreme case. The command gains were weighted according to Eq. (9).*

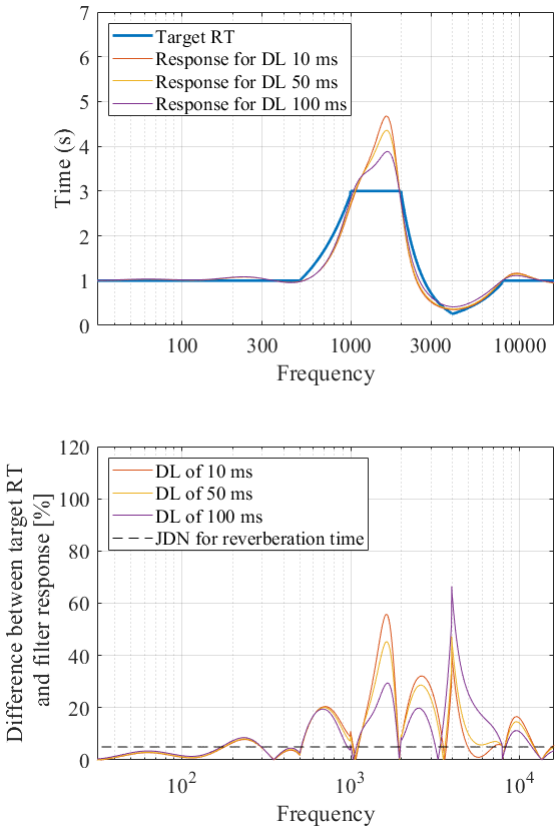

Figure 11: *(Top) Target reverberation time and reverberation time obtained with the GEQ for three different delay-line lengths for the artificial extreme case after gain weighting. (Bottom) Difference expressed as a percentage of the obtained reverberation time deviation from target values. Cf. Fig. 9.*

line length. In the end, all delay lines displayed similar differences from target values, which is a huge improvement from before the optimization.

3.3. Comparison with previous method

The proposed method was compared with the design presented in [13], which solves the nonlinear least-squares problem based on the T_{60} least-squares problem, as given in Eq. (11), with additional constraints on the command gains. The abbreviation TLSCon in Tables 3 and 4 refers to the results obtained with this method. To allow direct comparison, the same reverberation time and delay-line length were chosen. The error percentage in T_{60} for each method are presented in Table 3.

The proposed method produces a smaller approximation error than the solution suggested in [13]. The largest deviation from the target value occurs at 4 kHz, where an attenuation of -60 dB is needed. However, the obtained 62.69% error is a huge improvement compared to the TLSCon solution error of 280% for the same frequency.

3.4. Computational complexity of the proposed design

The GEQ with the first-order high-shelf filter used in the present work was compared in terms of computational cost with three other graphic equalizers: the proportional graphic equalizer (TLSCon) [13,16], the cascaded fourth-order equalizer (EQ4) [19], and the high-precision parallel equalizer (PGE) [17, 20]. The values are given for filter configurations as stated in [15] and are presented together with the number of operations for the proposed design in Table 4.

The design proposed in the present work requires less computation than the cascaded fourth-order equalizer and the high precision parallel equalizer. It needs a few more operations than the proportional graphic equalizer because the first-order high-shelf filter has been inserted to process frequencies above 16 kHz.

4. CONCLUSIONS

The present work investigated the effect of using a cascaded GEQ with a first-order high-shelf filter as the attenuation filter in the FDN. In order to evaluate the performance of the proposed design, two cases, a real-life case of an existing concert hall's reverberation time T_{60} and an artificially created extreme case, were tested. Additionally, weighted-gain optimization was performed to improve the results. The new weighting matrix emphasizes the approximation error occurring close to 0 dB. The gains are then determined by minimizing relative error between the filter response and the target reverberation time.

Table 3: *Error percentage for T_{60} approximated using the previous method (TLSCon) and the proposed method.*

Center frequency	63 Hz	125 Hz	250 Hz	500 Hz	1 kHz	2 kHz	4 kHz	8 kHz	16 kHz
TLSCon [13]	**1.00%**	**0.00%**	**3.00%**	**2.00%**	**9.00%**	**32.00%**	280.00%	31.00%	5.00%
Proposed method	3.39%	1.44%	8.15%	2.54%	16.98%	49.24%	**62.59%**	**20.69%**	**4.98%**

Table 4: *Number of operations per output sample for octave band equalizers.*

Design	ADD	MUL	TOTAL
TLSCon	40	50	90
EQ4	140	150	290
PGE	80	81	161
Proposed	42	52	94

The proposed method was shown to perform an excellent approximation of the real-life reverberation time values, resulting in an error between the target and obtained values that is lower than the JND. When the desired values change dramatically between neighboring frequency bands, the presented algorithm causes greater errors in the reverberation time, which can be then considerably reduced by the weighted-gain optimization. The study showed that the proposed method produces a smaller approximation error in the reverberation time than previous methods, and its computational cost is low or about the same compared to other designs.

The plans for further development of this work include providing subjective evaluation of the results as well as incorporating the proposed attenuation filter and the weighted-gain optimization method in other tools for creating artificial reverberation.

5. REFERENCES

[1] H. P. Seraphim, "Untersuchungen über die Unterschiedsschwelle exponentiellen Abklingens von Rauschbandimpulsen," *Acta Acustica united with Acustica*, vol. 8, no. 4, pp. 280–284, 1958.

[2] M. G. Blevins, A. T. Buck, Z. Peng, and L. M. Wang, "Quantifying the just noticeable difference of reverberation time with band-limited noise centered around 1000 Hz using a transformed up-down adaptive method," in *Proc. Int. Symp. Room Acoustics (ISRA)*, Toronto, Canada, June 9–11, 2013.

[3] M. Karjalainen and H. Järveläinen, "More about this reverberation science: Perceptually good late reverberation," in *Proc. 111th Audio Eng. Soc. Conv.*, New York, USA, Sept. 21–24, 2001.

[4] ISO, "ISO 3382-1, Acoustics – Measurement of room acoustic parameters – Part 1: Performance spaces," Tech. Rep., 2009.

[5] J. M. Jot and A. Chaigne, "Digital delay networks for designing artificial reverberators," in *Proc. 90th Audio Eng. Soc. Convention*, Paris, France, Febr. 19–22, 1991.

[6] V. Välimäki, J. D. Parker, L. Savioja, J. O. Smith, and J. S. Abel, "Fifty years of artificial reverberation," *IEEE Trans. Audio Speech Lang. Process.*, vol. 20, no. 5, pp. 1421–1448, Jul. 2012.

[7] S. J. Schlecht and A. P. Habets, "On lossless Feedback Delay Networks," *IEEE Trans. Signal Process.*, vol. 65, no. 6, pp. 1554–1564, Mar. 2017.

[8] J. Moorer, "About this reverberation business," *Computer Music J.*, vol. 3, no. 2, pp. 13–28, 1979.

[9] J. M. Jot, "Efficient models for reverberation and distance rendering in computer music and virtual audio reality," in *Proc. Int. Computer Music Conf.*, Thessaloniki, Greece, Sept. 1997.

[10] T. Wendt, S. van de Par, and S. D. Ewert, "A computationally-efficient and perceptually-plausible algorithm for binaural room impulse response simulation," *J. Audio Eng. Soc.*, vol. 62, no. 11, pp. 748–766, Nov. 2014.

[11] M. Holters and U. Zölzer, "Parametric high-order shelving filters," in *Proc. 14th European Signal Processing Conference (EUSIPCO)*, Florence, Italy, Sept. 4–8, 2006.

[12] J.-M. Jot, "Proportional parametric equalizers–Application to digital reverberation and environmental audio processing," in *Proc. 139th Audio Eng. Soc. Conv.*, New York, USA, Oct. 29–Nov. 1, 2015.

[13] S. J. Schlecht and A. P. Habets, "Accurate reverberation time control in Feedback Delay Networks," in *Proc. Digital Audio Effects (DAFx-17)*, Edinburgh, UK, Sept. 5–9, 2017, pp. 337–344.

[14] S. J. Orfanidis, *Introduction to Signal Processing*, Rutgers Univ., Piscataway, NJ, USA, 2010.

[15] V. Välimäki and J. Liski, "Accurate cascade graphic equalizer," *IEEE Signal Process. Lett.*, vol. 24, no. 2, pp. 176–180, Feb. 2017.

[16] R. J. Oliver and J. M. Jot, "Efficient multi-band digital audio graphic equalizer with accurate frequency response control," in *Proc. 139th Audio Eng. Soc. Conv.*, New York, USA, Oct. 29–Nov. 24, 2015.

[17] V. Välimäki and J. Reiss, "All about audio equalization: Solutions and frontiers," *Applied Sciences*, vol. 6, no. 5, May 2016.

[18] B. Bank and V. Välimäki, "Robust loss filter design for digital waveguide synthesis of string tones," *IEEE Signal Process. Lett.*, vol. 10, no. 1, pp. 18–20, Jan. 2003.

[19] M. Holters and U. Zölzer, "Graphic equalizer design using higher-order recursive filters," in *Proc. Int. Digital Audio Effects (DAFx-06)*, Montreal, Canada, Sept. 18–20, 2006, pp. 37–40.

[20] J. Rämö, V. Välimäki and B. Bank, "High-precision parallel graphic equalizer," *IEEE/ACM Trans. Audio Speech Lang. Process.*, vol. 22, no. 12, pp. 1894–1904, Dec. 2014.